Spiral Wave Dynamics under Pulsatory Modulation of Excitability

ARTICLE *in* THE JOURNAL OF PHYSICAL CHEMISTRY · DECEMBER 1996

Impact Factor: 2.78 · DOI: 10.1021/jp9616674 · Source: OAI

3 AUTHORS, INCLUDING:

Vladimir Zykov
Max Planck Institute for Dynamics and Self-O…
120 PUBLICATIONS **2,298** CITATIONS
SEE PROFILE

Stefan C Müller
Otto-von-Guericke-Universität Magdeburg
288 PUBLICATIONS **5,024** CITATIONS
SEE PROFILE

Spiral Wave Dynamics under Pulsatory Modulation of Excitability

S. Grill,† V. S. Zykov,† and S. C. Müller*,†,‡

Max-Planck-Institut für molekulare Physiologie, D-44139 Dortmund, Germany, and Institut für Experimentelle Physik, Otto-von-Guericke-Universität, Universitätsplatz 2, D-39106 Magdeburg, Germany

Received: June 6, 1996; In Final Form: August 29, 1996[⊗]

The dynamics of meandering spiral waves in the photosensitive Belousov−Zhabotinsky reaction is investigated under external forcing by single light pulses, periodic pulses, and feedback-controlled sequences of light pulses. The effect of a single stimulus on the trajectory of the spiral tip is related to the phase of the tip motion on the trajectory at the moment when the stimulus is applied. Periodic stimulation of the medium can produce spiral wave entrainment and resonance. A connection between the phase of the stimuli and the stability of the regime of entrainment is shown. In the feedback-controlled system each stimulus is applied at a moment corresponding to the passage of a wave front through a particular detection point. The introduction of such a feedback results in two new dynamic regimes, the entrainment and resonance attractor. Size and stability of these attractors are determined by the value of a time delay in the feedback loop. The experimental results are corroborated by numerical simulations performed with a modified two-component Oregonator model.

1. Introduction

Spreading excitation waves are observed in a great variety of reaction−diffusion systems such as Xenopus Laevis oocytes,[1] aggregating slime mold cells,[2] CO oxidation on platinum surfaces,[3] neuronal tissue like chicken retina,[4] cardiac muscle tissue,[5,6] and chemical systems like the Belousov−Zhabotinsky (BZ) reaction.[7−9] Among these systems, the BZ reaction is most suitable for the observation and reproduction of excitation waves and for the effects of external influence on them. Considering the similarity of the underlying mechanisms of wave propagation in these excitable media, results obtained for the dynamics of excitation waves in the BZ reaction can often be qualitatively transferred to other reaction−diffusion systems. Typically, in these systems rotating spiral waves are the most persistent form of spatiotemporal patterns of excitation. In some biological cases, like cardiac muscle tissue, the occurrence of spiral waves leads to severe malfunction;[6] in others, like the slime mold *Dictyostelium discoideum*, it is indispensable for the reproduction and survival of the species.[2] With these examples in mind, the idea to develop appropriate means to control the dynamics of spiral-shaped excitation waves by external influences constitutes an interesting problem with potential biological applications.

In our experiments we use the BZ reaction with the light-sensitive catalyst $Ru(bpy)_3^{2+}$ which allows to control effectively the excitability and therefore the dynamics of the system by external illumination.[10−16] In particular, the trajectory of the tip of a spiral wave, which is an important characteristic of the spiral wave motion, is very sensitive to changes of external illumination. Under constant, uniform illumination the shape of the trajectory strongly depends on the applied light intensity.[13] Under sinusoidal modulation of illumination a synchronization of the movement of the spiral tip with the external frequency within entrainment bands,[12,13] a resonance drift of the spiral core,[14,15] and irregular motions of the tip[14] are observed. If a feedback mechanism is introduced by adjusting the period of a pulsatory modulation to the measured wave period at a particular detection point of the system, two new dynamic regimes named entrainment and resonance attractor are found.[16]

It is desirable to compare the effects of a periodic stimulation with those obtained for a feedback mechanism. Unfortunately, a direct comparison between the results obtained in refs 12−15 and ref 16 is not possible, because different temporal profiles were used for the external forcing. Another interesting problem is to investigate the effect of single-impulse perturbation as a prerequisite to obtain the large variety of spiral tip trajectories under pulsatory modulation of excitability.

With these goals in mind, we examine in this work the dynamics of spiral waves under a single, a periodic, and a feedback-controlled pulsatory modulation of global excitability. The pulsatory modulation is achieved by the repetitive application of short "light pulses" with a standard shape to the photosensitive medium. While the study of single-pulse forcing and periodic pulsatory modulation is completely new, the investigation of the feedback system mechanism is a direct continuation of previous work,[16] in that we essentially extend our former results by a detailed investigation of the role of a time delay in the feedback loop.

2. Experimental Setup

The BZ reaction is realized in a thin layer (0.7 mm) of silica gel in a petri dish (diameter 7 cm).[12] The catalyst $Ru(bpy)_3^{2+}$ (4.2 mM) is immobilized in the gel.[17] After BZ solution (18 mL) is poured onto the gel, equilibrium between gel and liquid layer is established within a few minutes, and the calculated concentrations of reactants (disregarding the bromination of malonic acid[18]) are 0.2 M $NaBrO_3$, 0.17 M malonic acid, 0.39 M H_2SO_4, and 0.09 M NaBr. The experiments are carried out at a temperature of 23 ± 1 °C, and the petri dish is covered by a glass lid to minimize the effects of atmospheric oxygen. The petri dish is illuminated through two polarization filters by white light (halogen lamp, 250 W), which serves to observe the patterns as well as to control the excitability. One of the two filters can be rotated by a computer-controlled step motor. This allows to generate any desired function of illumination intensity within a range of 0.01−2.22 mW/cm^2.[16] For all experiments

* To whom correspondence should be addressed.
† Max-Planck-Institut für molekulare Physiologie.
‡ Otto-von-Guericke-Universität.
⊗ Abstract published in *Advance ACS Abstracts,* November 1, 1996.

S0022-3654(96)01667-X CCC: $12.00

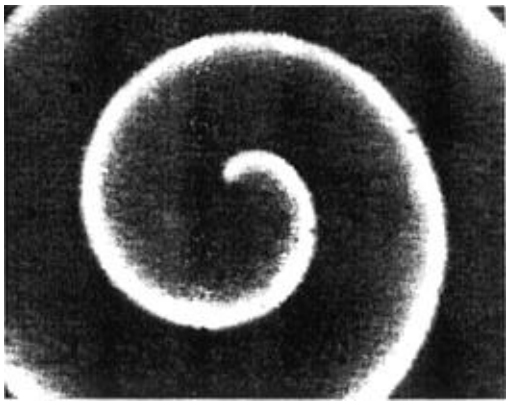

Figure 1. Central part of a spiral wave in the ruthenium-catalyzed BZ reaction observed under constant background intensity of illumination. Picture size: 6.1 × 5.8 mm.

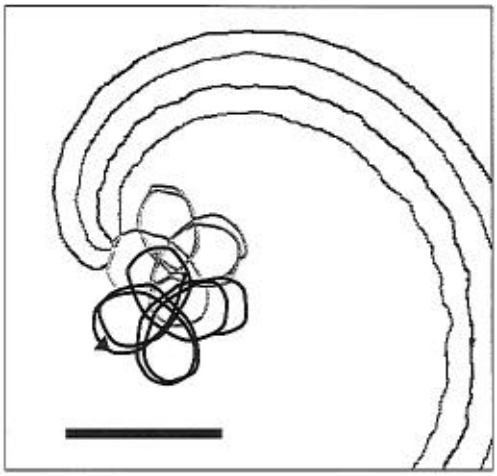

Figure 2. Overlay of two contour lines of a spiral wave extracted from two consecutive frames of a movie (time interval 1.56 s). The tip is defined as the intersection of the two contour lines. In addition, the four-lobed trajectories of the spiral wave tip observed for the constant background intensity of illumination before (in gray) and after (in black) application of a single light pulse are shown. Scale bar: 0.5 mm.

the "background intensity" was set to 0.5 mW/cm^2 and short "light pulses"—an increase of global illumination intensity to 1.5 mW/cm^2 for 5 s—are triggered once, periodically, or by a feedback mechanism described below. Any intensity jump itself consists of 150 single steps of the motor and lasts for 0.54 s. The transmitted light is detected by a CCD camera at a wavelength of 490 nm, which is near the maximum difference of absorption between the oxidized and the reduced state of the catalyst (at 460 nm). Concentration waves of the oxidized catalyst appear as bright bands on a dark background. The pictures are digitized by an image acquisition card, analyzed on-line, and also stored on a video recorder.[19]

At the beginning of each experiment a single, unperturbed spiral wave (see Figure 1) is created in the center of the dish by breaking a spontaneously arising circular wave front with a thin laser beam (diameter 1 mm) and shifting one of the two originating open ends to the boundary of the dish.[20]

The position of the tip is detected automatically, which allows to determine the tip trajectory objectively for a long period of time and analyze a vast number of experiments quantitatively. The detection method is based on the overlay of appropriate contour lines of the spiral wave extracted from two consecutive frames of a movie (time step 1.56 s). The intersection point of these two contour lines is defined as the actual tip location[21] (see Figure 2). It corresponds to the point where the concentration of the oxidized catalyst has not changed between the two frames of observation and is therefore considered as the momentary center of rotation. The trajectory of the tip is then obtained by connecting the temporal sequence of thus detected tip locations.

Under the given experimental conditions the trajectory of the tip looks like a hypocycloid (cf. Figure 2). This compound trajectory can be considered as a superposition of two circular motions with different radii and rotational frequencies[22,23] in contrast to a rigid rotation where the tip rotates with a constant frequency on a circular pathway with a fixed center. Moreover, in our case the meander of the trajectory is so pronounced that the spiral wave front passes periodically through the symmetry center of the trajectory. While for rigid rotation the concentration measured at the symmetry center is constant, it is a periodic function of time in the considered case. The oscillation period in the center of the tip trajectory is measured to be $T_0 \approx 25$ *s*. The average period of the oscillations at a point far away from the center is $T_\infty \approx 33$ *s*. This difference reflects the two-frequency dynamics of the meandering spiral wave. Generally speaking, the period T_0 can be expressed as $T_0 = T_\infty(n - 1)/n$, where n is the number of lobes of the hypocycloid (not necessarily integer).[14] We prefer to use the periods T_0 and T_∞ as independent quantities because they can be measured easily and used directly in the following analyses. The number n can then be calculated by using the above relationship.

3. Experimental Results

As shown in Figure 2 (gray curve), the trajectory of a spiral tip in a BZ layer illuminated by a constant and spatially homogeneous background intensity of 0.5 mW/cm^2 is a hypocycloid with approximately four lobes. Its shape and size remain unchanged for more than 2 h. If a single stimulus in form of a light pulse is applied, the trajectory is perturbed. However, the tip quickly approaches a new, similar trajectory after the stimulus is over. This trajectory is shifted and, in general, rotated with respect to the initial one (black curve in Figure 2).

The parameters describing the effect of a single stimulus on the trajectory depend on the phase of the tip motion at the instant, when the stimulus is applied. To specify this phase, we divide the four-lobed trajectory into single lobes, which begin and end at the respective points closest to the symmetry center of the trajectory. Each point of a single lobe is specified by the time passed, since the tip has entered the lobe. This time, normalized by the time to complete the whole lobe (which is exactly equal to the period T_0), is defined as the phase ξ within the lobe. The angle between the directions of the tip motion at the beginning and at the end of one lobe α is equal to $360°/n$ (in our case $\alpha \approx 90°$). Obviously, a stimulus applied at the same phase for two neighboring lobes should result in a similar deformation of the unperturbed trajectory, but the direction of the shift will be turned on the angle α. The deformation of the trajectory after a single light pulse can be specified by several parameters. We start with the distance d between the centers of the unperturbed and the "new" trajectory, or the amplitude of the shift, as shown in Figure 3a. The maximum shift is observed, when the stimulus is applied at a phase of $\xi = 0.25$, and the minimum shift occurs at phases near $\xi = 0.75$. The direction of the shift ϑ—relative to the direction of the tip motion at the moment when the stimulus is triggered—is shown in Figure 3b. For the angle ϑ, measured against the sense of rotation of the spiral tip between the tangent of the motion and the direction of the shift, only values between 10° and 100° occur. The maximum angle ϑ is observed at a phase of $\xi = 0.65$, and the minimum of ϑ is found at a phase between $\xi = 0.85$ and $\xi = 0.1$. The angle ψ of rotation of the new trajectory

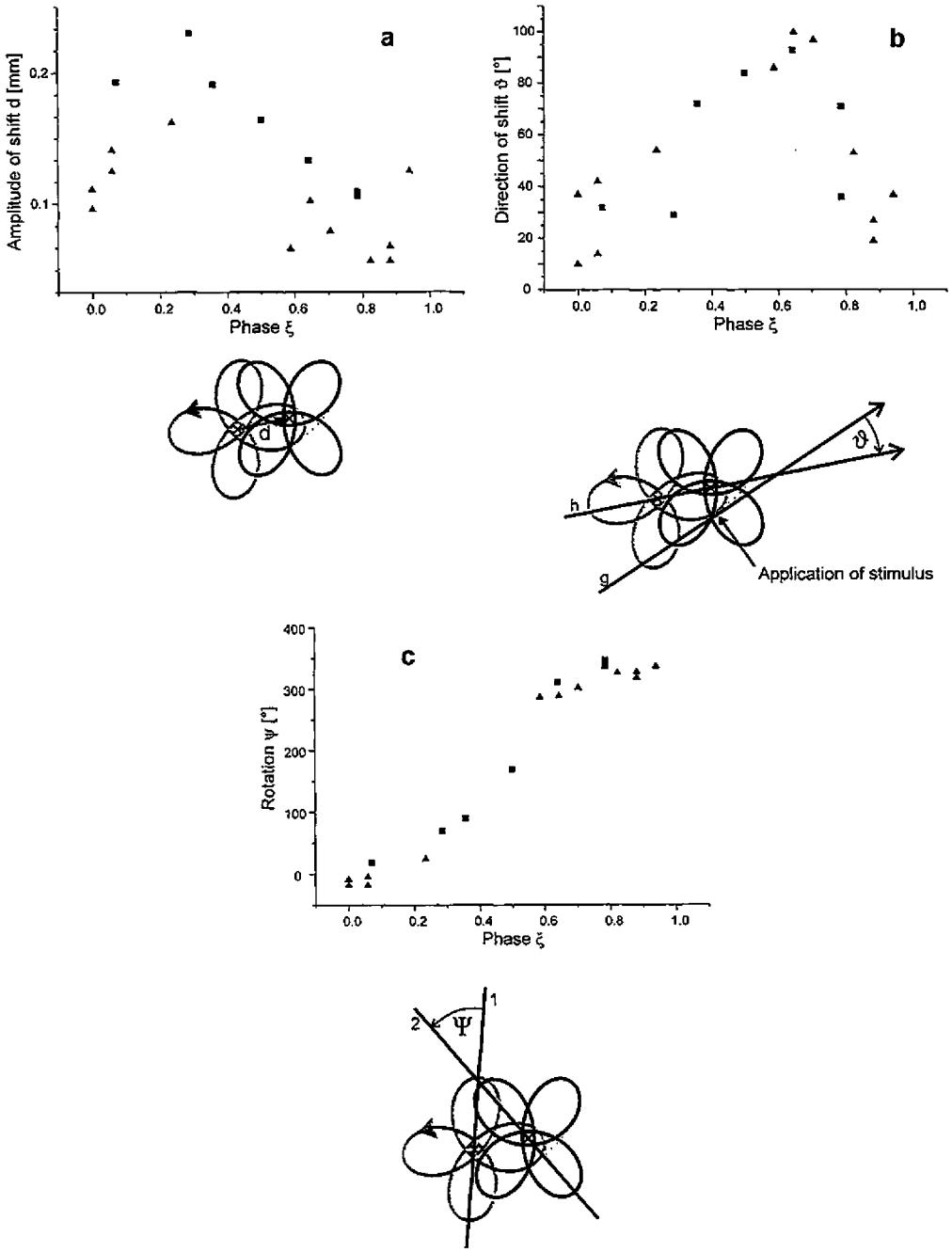

Figure 3. Effect of a single stimulus on the trajectory of the spiral tip as a function of the phase ξ of application. (a) Spatial shift of the trajectory's symmetry center; (b) direction of the shift; (c) rotation of the trajectory. Symbols □ and △ represent data from two separate experiments. Below each graph a symbolic sketch of the trajectories is drawn, and the measured parameters are indicated.

relative to the previous one is shown in Figure 3c. If the stimulus is triggered at a phase between $\xi = 0.7$ and $\xi = 0.2$, the orientation of the two trajectories differs only little ($\psi = 0°$ or 360°). At phases ranging from $\xi = 0.2$ to $\xi = 0.7$ the angle ψ of rotation increases monotonously with growing phase.

For a periodic sequence of stimulating light pulses the induced alterations of the trajectory, especially the shift of the spiral wave core, will accumulate over a period of time. Depending on the stimulating period quantitatively different phenomena occur.

In analogy to the findings for sinusoidal stimulation,[12−14] a synchronization of the tip motion with the external frequency as well as a resonance drift of the spiral core is observed. In our experiments, we find several entrainment bands, each characterized by a rational number *r/s*, where *r* is the number of lobes completed during *s* periods of external modulation. The positions of the 1/2, 1/1, and 2/1 band on the axis of modulation period are shown in Figure 4 together with illustrations of corresponding trajectories. While the 1/2 entrainment band at a value around $T_m/T_0 = 0.5$ is very narrow, the 1/1 band stretches from $T_m/T_0 = 0.90$ (relatively compact, three-lobed trajectory) to $T_m/T_0 = 1.25$ (relatively spread, seven-lobed trajectory). The 2/1 band is located between $T_m/T_0 = 2.05$ and $T_m/T_0 = 2.25$. All these bands are shifted to slightly higher modulation periods with respect to the intuitively expected periods of $T_m/T_0 = 0.5$, $T_m/T_0 = 1.0$, and $T_m/T_0 = 2.0$, because each stimulus should reduce the angular velocity of the tip motion which results in a slight increase of the period T_0 with respect to the unperturbed system. Within the 1/1 and 2/1 band there is a prononced shift of the phase of the stimuli. Within the 1/1 band the phase is shifted from $\xi = 0.7$ at the period $T_m/T_0 = 0.90$ to $\xi = 0.15$ at the period $T_m/T_0 = 1.25$. Within the 2/1 band the phase is shifted from $\xi = 0.9$ at the period $T_m/T_0 = 2.05$ to $\xi = 0.25$ at the period $T_m/T_0 = 2.25$.

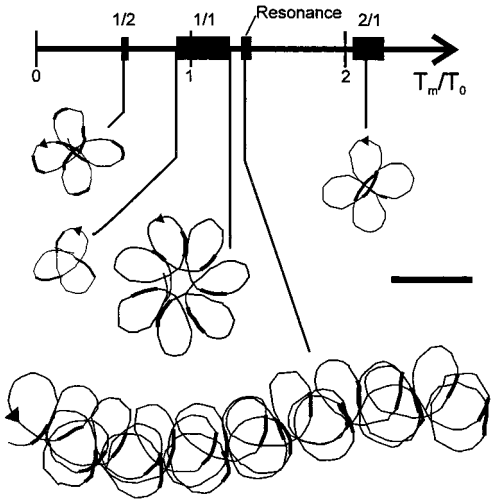

Figure 4. Observed bands of entrainment (1/2, 1/1, 2/1) and resonance along the axis of normalized modulation period. Representative trajectories of the bands are shown. Thick segments of the trajectories indicate the application of light pulses. Scale bar: 0.5 mm.

The resonance condition is fulfilled, if the spiral is stimulated with the wave period T_∞ measured far from the center.[14] Note that the direction of the tip motion is changing with this period. Hence, one can expect to observe a resonance drift if the application of external disturbances corresponds to a given direction of the tip motion. Indeed, at a modulation period of $T_m/T_\infty = 1.03$ the spiral core undergoes a resonance drift. The spiral core is shifted in one direction, but in contrast to the case of entrainment, no synchronization with the external signal occurs. This is natural because in this case the modulation period differs sufficiently from the period of one lobe ($T_m/T_0 = 1.37$), and consequently the phase of external pulses varies from lobe to lobe. The range of external periods corresponding to this regime of resonance is very narrow: already at periods of $T_m/T_\infty \leq 0.99$ and $T_m/T_\infty \geq 1.04$ resonance could not be observed any more. Even small changes in the system dynamics, e.g., due to aging, can change the wave period T_∞ so that in these experiments the resonance regime by periodic stimulation cannot be maintained over long times without adjusting the modulation period frequently.

In further experiments, we introduced a feedback mechanism which makes it possible to adjust the period of global modulation to the wave period measured at a particular detection point. The intensity of the transmitted light at the detection point (typically a 3×3 pixel area selected on the digitized video image) is determined on-line with a time step of 0.02 s. The passage of a wave front is indicated by a quick rise of the transmitted light intensity and detected automatically. Each time a wave front reaches the detection point a single stimulus of 5 s duration is triggered immediately or with a certain time delay τ after the wave front passage. Note that the detection point is not an inhomogeneity of the system itself but is just the point where the pictures of the CCD−camera are analyzed.

Under these feedback conditions two dynamic regimes, called the entrainment and resonance attractor, are observed as reported already in ref 16 and illustrated by several examples in Figures 5 and 6. In both cases the chosen detection point is the symmetry center of the asymptotic tip trajectory.

The entrainment attractor is observed if the detection point is located close to the center of the initial, unperturbed trajectory. A modulation period of $T_m \approx T_0$ is triggered, and the tip moves synchronously with the external signal. For larger distances between the detection point and the unperturbed trajectory, the tip is found to move on the resonance attractor. Then, there is no synchronization any more, but still the spiral core drifts along a large circle. Due to the large distance between spiral tip and detection point, the average period of the triggered stimuli is close to T_∞, which is the resonance period for the case of periodic modulation (cf. Figure 4).

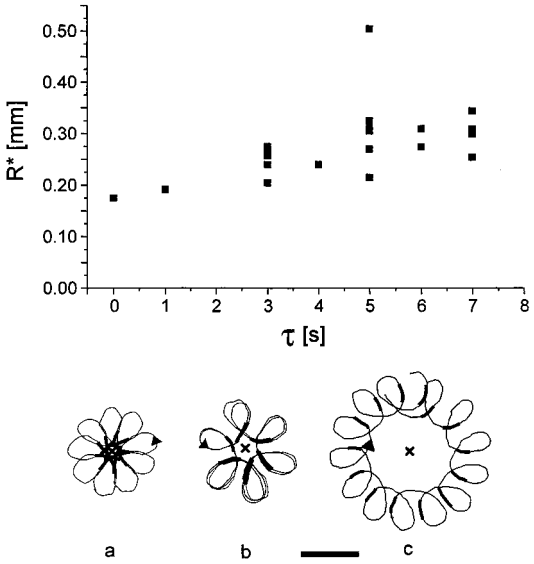

Figure 5. Entrainment attractor for different time delays τ. The upper part shows the mean value R^* of inner and outer radius of the attractor as a function of time delay τ. For values of τ exceeding $\tau = 7$ *s* the entrainment attractor is not observed. Three trajectories are shown in the lower part: (a) $\tau = 0$ s, (b) $\tau = 3$ s, and (c) $\tau = 5$ s. Thick segments of the trajectories indicate the application of light pulses. Scale bar: 0.5 mm.

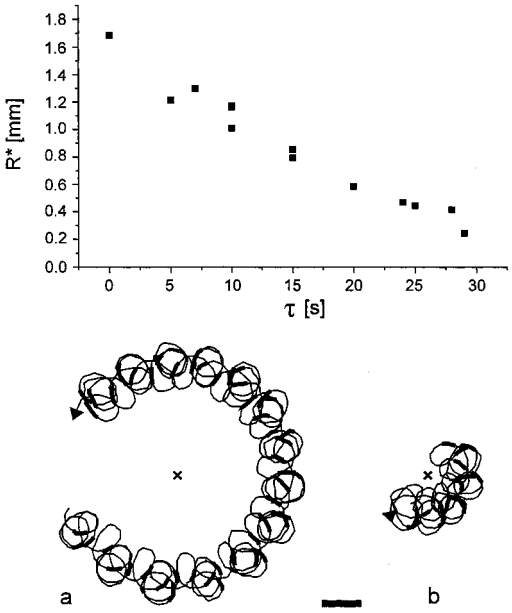

Figure 6. Resonance attractor for different time delays τ. The upper part shows the mean value R^* of inner and outer radius of the attractor as a function of time delay τ. Two trajectories are shown in the lower part: (a) $\tau = 7$ s and (b) $\tau = 25$ s. Thick segments of the trajectories indicate the application of light pulses. Scale bar: 0.5 mm.

For both attractors the requested conditions for synchronization ($T_m \approx T_0$) and resonance ($T_m \approx T_\infty$), respectively, are self-stabilizing. Both regimes are stable with respect to a small shift of the detection point: the center of the attractor follows the shift.

The above-described phenomena occur when there is no time delay between the registration of the wave front at the detection point and the triggering of the stimulus. The introduction of a time delay τ into the feedback loop leads to a drastic change of the shape of the attractors as well as the set of initial conditions

determining which attractor finally governs the spiral tip motion. With increasing time delay τ the radius R^* of the entrainment attractor and the number of lobes of the pattern increase (see Figure 5). Irrespective of shape and size of the attractor, the synchronization is preserved. Only the phase of the tip motion at which the stimuli are triggered is shifted markedly from $\xi = 0.95$ ($\tau = 0$ s) to $\xi = 0.15$ ($\tau = 5$ s) (Figure 5). This observation is a direct analogy to the behavior within the 1/1 entrainment band for periodic stimulation, where a similar connection between the phase ξ of the stimuli and the size of the trajectory is found. If the delay is chosen larger than a certain value ($\tau = 5-7$ s), the synchronization breaks down and only the resonance attractor is observed, even for very small distances between the detection point and the unperturbed trajectory.[16]

The shape and size of the resonance attractor also change with increasing time delay τ (see Figure 6). The radius R^* decreases with increasing τ from $R^* = 1.64$ mm ($\tau = 0$) to $R^* = 0.25$ mm ($\tau = 29$ s). The behavior of the resonance attractor for time delays exceeding $\tau = 29$ s could not be investigated, because the delay is then close to the wave period at the detection point, and it is not possible to determine the passage of a wave front at the detection point while the system is being stimulated.

4. Simulation

We complemented the experiments by numerical simulations of the observed phenomena. For this purpose we used an extension of the Oregonator model.[24,25] It includes an additional term $\phi = \phi(t)$ taking into account the additional bromide production that is induced by the external illumination of the system:[12,14]

$$\frac{\partial u}{\partial t} = \nabla^2 u + \frac{1}{\epsilon}\left[u - u^2 - (fv + \phi)\frac{u - q}{u + q}\right] \qquad (1a)$$

$$\frac{\partial v}{\partial t} = u - v \qquad (1b)$$

The variables u and v correspond to the concentrations of the autocatalytic species $HBrO_2$ and the catalyst, respectively. The parameters $\epsilon = 0.05$, $q = 0.002$, and $f = 2.0$ were fixed. In the function $\phi(t)$ the "light pulses" are simulated as a sequence of impulses with amplitude A and duration D, which are added to a background flow $\phi_0 = 0.01$.

In our calculations we fixed the duration to $D = 0.3$ and studied the trajectories of the spiral wave tip for different values of the amplitude A and the period T_m. The computations were performed by the explicit Euler method, using the five-point approximation of the Laplacian on a 380×380 array with a grid spacing $\Delta x = 0.1$ and time steps $\Delta t = 0.001$.

A single spiral was induced by a special choice of initial conditions for the system (1). For zero amplitude A of the stimulus one can observe the unperturbed trajectory which is close to a five-lobed hypocycloid with a wave period $T_\infty = 3.6$ Oregonator time units measured far away from the symmetry center. A different period $T_0 = 2.8$ is measured at the symmetry center of the unperturbed trajectory.

If the stimulating period is close to T_0, the movement of the tip can be synchronized even by a very small external perturbation. Within this fundamental synchronization band one external pulse corresponds to one lobe of the resulting trajectory. The width of the synchronization band grows with the amplitude A as shown in Figure 7. The external forcing affects both the shape and the period of the unperturbed trajectory. These variations become more pronounced with increasing amplitude. For instance, the number of the lobes of the resulting trajectory varies from 2.5 up to 12 for the amplitude $A = 0.02$. Of course,

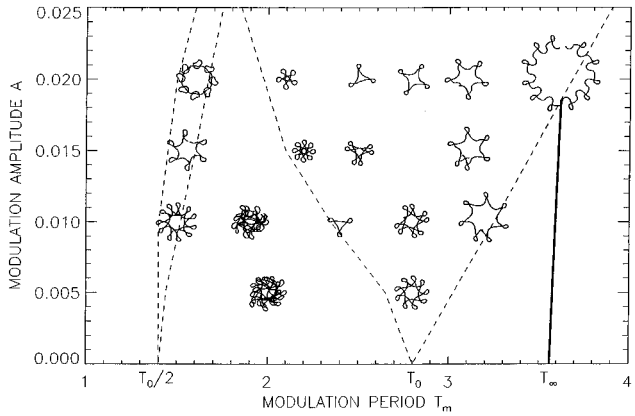

Figure 7. Tip trajectories calculated for model (1) as a response to pulsatory modulation of the additional bromide production. Trajectories are shown in the plane spanned by the amplitude A and period T_m of modulation. Dashed lines mark boundaries of entrainment bands with winding number 1/2 and 1/1. The thick, almost vertical bar indicates the region of primary resonance.

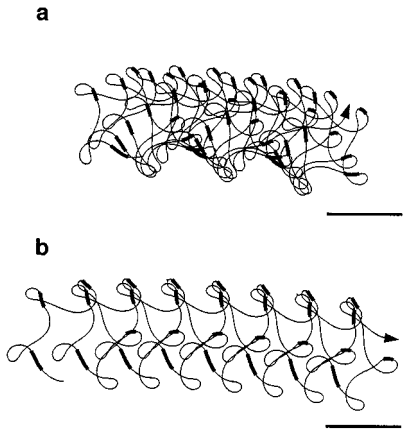

Figure 8. Resonance drift of a spiral wave computed for model (1) with the following modulation parameters: (a) $T_m = 3.58$, $A = 0.005$ and (b) $T_m = 3.6$, $A = 0.01$. The computed time interval is (a) $T = 150$ and (b) $T = 100$. Thick segments of the trajectories correspond to the application of light pulses. Scale bar: 5.0 Oregonator space unit.

the phases of application of the external impulses vary within the boundaries of the entrainment band.

Another synchronization band with two external pulses per one lobe is shown in the left part of Figure 7. This band is narrow with respect to the fundamental one. Its root corresponds to the modulation period $T_m = T_0/2$. Trajectories observed between these two bands look rather irregular, because they include many different frequencies.

The resonance drift of the spiral wave core is computed for modulation periods close to T_∞ (thick solid line in Figure 7). Two trajectories observed in this region are shown in Figure 8. The velocity of the observed drift is proportional to the external amplitude in accordance with the kinematical theory of the resonance drift.[26] However, this theory considers a circular trajectory (rigid rotation of a spiral wave) as an unperturbed one and predicts a looping line as the resulting resonance trajectory. In our case a multilobed trajectory is perturbed by a periodic sequence of pulses, and there are more possibilities for the resulting trajectories. For instance, a drift of the symmetry center of the unperturbed trajectory together with its rotation result in the trajectory shown in Figure 8a. In contrast to entrainment, the phases of external pulses vary for different lobes, and hence, no synchronization occurs. Still, however, the resulting trajectory is well ordered.

An increase of the external amplitude not only increases the drift velocity but also leads to some kind of synchronization.

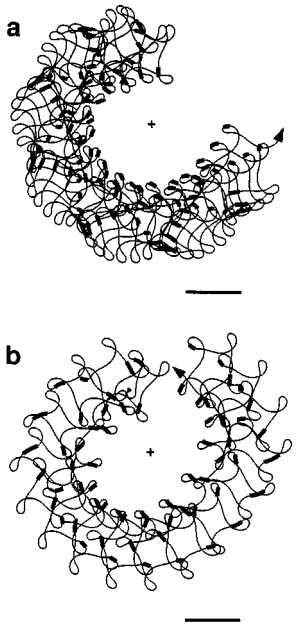

Figure 9. Resonance attractor computed for model (1) with two different amplitudes A of the pulses in the feedback loop: (a) $A = 0.002$; (b) $A = 0.01$. The computed time interval is (a) $T = 360$ and (b) $T = 240$. The time delay is $\tau = 2.0$. Thick segments of the trajectories correspond to the application of light pulses. Scale bar: 5.0 Oregonator space unit.

Indeed, the trajectory in Figure 8b can be treated as a translation of a five-lobed segment along a straight line. This segment is described during four external pulses. The phase of the external influence is different for each of these five lobes, but the periodicity of the whole process is clear. Therefore, we have in this case an entrainment with 5:4 locking. Still further increasing the pulse amplitude finally leads to full 1:1 synchronization. The resulting trajectory is shown in the upper right corner of Figure 7.

The following part of our computation is devoted to the simulation of a system with a feedback. In analogy to the experimental study, an external pulse is applied with a time delay τ after the passage of the wave fronts through a particular detection point. Two attractors have been computed earlier in such a system.[16] The present computations demonstrate the role of the amplitude of the external signal.

We start with a spiral tip moving on a five-lobed hypocycloid. If the center of the unperturbed spiral wave is located rather far away from the detection point, the center of the hypocycloid moves and describes a large circle around the detection point even for a very small amplitude A of external influence (Figure 9a). For larger amplitudes A the radius of the circular motion remains practically the same, while the velocity of the drift is proportional to the amplitude (Figure 9b). No synchronization takes place between external impulses and the tip motion. The mean value of the pulse−pulse interval is close to $T = T_\infty$. All these properties are specific for the resonance drift and on this background the asymptotic tip trajectory is called "resonance attractor".

If the detection point is placed near the symmetry center of the unperturbed trajectory, another attractor is computed. The symmetry center is attracted to the position of the detection point after some transient process, and then it ceases to move. In this stationary regime the front of the wave passes through the center with a period close to T_0. The value of the period and the shape of the trajectory depend on the amplitude of external perturbation and the time delay τ. The crucial role of the time delay was discussed earlier in ref 16. Two examples of the stationary trajectory computed for two different amplitudes A are shown in Figure 10. A small amplitude results in a negligible transformation of the unperturbed trajectory (Figure 10a). An increase of the amplitude induces a more pronounced deformation (Figure 10b). All trajectories observed for this entrainment attractor can be found within the family of trajectories which belong to the fundamental entrainment band (Figure 7).

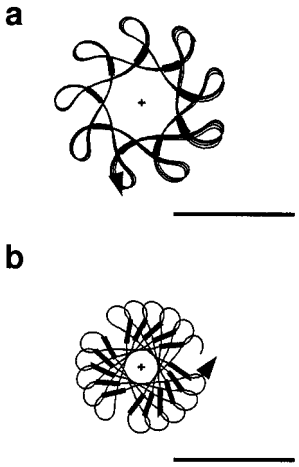

Figure 10. Stationary trajectories of entrainment attractors computed for model (1) with two different amplitudes A of the pulses in the feedback loop: (a) $A = 0.002$; (b) $A = 0.01$. The time delay is $\tau = 2.0$. Thick segments of the trajectories correspond to the application of light pulses. Scale bar: 5.0 Oregonator space unit.

Thus, the model computations confirm the experimental observation of the effect of a pulsatory modulation and help to explain a relationship between the entrainment and the resonance phenomena as well as between a periodical and a feedback-controlled stimulation.

5. Discussion

A variety of well-defined spatiotemporal patterns have been shown to form in a thin layer of the BZ reaction perturbed by short light pulses. Our findings show that the pulsatory modulation of excitability is an effective means to control wave processes in excitable media.

We started a systematic study of the pulsatory modulation by investigating the effect of a single pulse on the wave dynamics. The changes of the location and orientation of the tip trajectory induced by a unique stimulation indicate that there is a clear dependency on the phase ξ of the tip motion at the moment when the stimulus is applied. Commonly, similar dependencies are used in the theory of nonlinear systems to predict the effect of a periodic modulation. However, in the considered distributed system the observed reaction to a single stimulus is much more complicated and includes not only a phase shift but a space shift and a rotation (see Figure 3). The elaboration of a corresponding theory is beyond the framework of this paper. However, the standard shape of a single pulse used in the present study results in new qualitative data which call for developing such a theory. The single pulse dependencies can be used, for instance, to study stability of the entrainment attractor.

The observed regimes of entrainment and resonance under periodic forcing are qualitatively the same as previously reported for a harmonic perturbation.[12−15] Therefore, the occurrence and properties of these regimes are not significantly connected with the particular shape of the applied periodic function of illumination intensity. The entrainment phenomenon emphasizes the important finding that the evolution of spiral waves in a distributed medium subject to periodic forcing resembles in many respects the dynamics of a periodically perturbed con-

centrated nonlinear oscillator. Indeed, the existence of entrainment bands including a complex structure of dynamical regimes within Arnold tongues is a typical property of many forced excitable systems.[27−29] The significance of the presented results lies in the fact that a family of unusual spatiotemporal patterns emerges, which can be used to control wave processes in active media.

The phenomenon of the resonance drift appears, in this context, as a characteristic feature of the dynamics of distributed systems. In contrast to entrainment, a temporal synchronization (phase locking) is not a specific condition for this regime. Nevertheless, the resulting trajectory is well-ordered in space. The experimental resonance trajectory presented in Figure 4 can be treated as a displacement in space of an elementary three-lobed fragment. Our computations (Figure 8) demonstrate that the number of lobes of an elementary fragment is a parameter related to the shape of the unperturbed trajectory and the intensity of the external perturbation. For a small external amplitude this elementary fragment looks like a slightly deformed unperturbed trajectory, and no synchronization occurs. An increase of the amplitude results in a smooth transition toward full synchronization. The resonance phenomena observed experimentally (Figure 4) or numerically (Figure 8) can be considered as quite simple scenarios of the resonance drift. More complicated regimes have been reported.[15]

The dynamics of the feedback-controlled medium exhibits also many qualitative features that are only possible for distributed systems. The feedback control allows to anchor a spiral core on attractive trajectories with a desired distance from the detection point and to shift the trajectories together with the detection point. Both the shape and the spatial location of the resulting tip trajectory can be manipulated by using relatively small, global perturbations. In previous studies, a spatial anchoring was only possible with relatively large, local perturbations like a laser spot.[20] Moreover, one can stabilize the regimes of resonance and synchronization over long periods of time, even if the parameters of the system like wave periods change, for example, due to aging processes.

The phase shift between the tip motion along a lobe and the application of the external pulse is essential, because it determines the shape of the resulting trajectory and its stability. Indeed, for the entrainment attractor the sequence of the external pulses is periodic, and the trajectories shown in Figure 5a−c belong to the family related to the 1/1 entrainment band plotted in Figure 4. As this entrainment band is traversed from left to right in this figure, the phase shift varies from $\xi = 0.7$ to $\xi = 0.15$, and the observed trajectory shape changes drastically. A similar variation of the trajectory shape (and of the phase shift) can be induced by increasing the time delay τ in the case of feedback-controlled stimulation (Figure 5). Obviously, in both of these cases the phase shift ξ determines the detailed shape of the trajectory. Moreover, the destabilization of the entrainment attractor for a rather long time delay corresponds to a specific phase shift ξ, in close analogy with the breakdown of the synchronization, when the right boundary of the entrainment band is crossed with growing modulation period. With periodic stimulation, however, an irregular motion of the spiral tip is observed if the stability of the entrainment is lost, whereas, under the feedback-controlled forcing, the tip approaches the resonance attractor as soon as the critical delay is exceeded and the stability of the entrainment attractor breaks down.

Numerical simulations with a rather general model convincingly confirm the experimental findings for the BZ reaction and show that the observed regimes are characteristic for excitable media of different nature. In addition, our computer experiments help to clarify the role of the amplitude of external stimuli. In particular, the diagram in Figure 7 allows to visualize the Arnold tongues, characterize periodic perturbations of spiral waves, and clarify the transition from the resonance drift to full synchronization. For the resonance attractor an increase of the amplitude results in an acceleration of the tip motion around the detection point without considerable influence on the general size of trajectory (Figure 9). On the other hand, for the entrainment attractor, the trajectory becomes more compact when the external amplitude is increased, as illustrated in Figure 10.

The opportunity to control the dynamics of spiral-shaped excitation waves by relatively small global perturbations could be transferred from the laboratory system BZ reaction to biological systems, and we suggest further experiments in this direction in the field of biological excitable media.

Acknowledgment. V.S.Z. acknowledges support from the WE-Heraeus-Stiftung, Hanau.

References and Notes

(1) Lechleiter, J.; Girard, S.; Peralta, E.; Clapham, D. *Science* **1991**, *252*, 123.
(2) Gerisch, G. *Naturwissenschaften* **1983**, *58*, 430.
(3) Jakubith, S.; Rotermund, H. H.; Engel, W.; von Oertzen, A.; Ertl, G. *Phys. Rev. Lett.* **1990**, *65*, 3013.
(4) Gorelova, N. A.; Bureš, J. *J. Neurobiol.* **1983**, *14*, 353.
(5) Allessie, M. A.; Bonke, F. I. M.; Schopman, F. J. G. *Circ. Res.* **1973**, *33*, 54.
(6) Davidenko, J. M.; Pertsov, A. V.; Salomonz, R.; Baxter, W.; Jalife, J. *Nature* **1992**, *355*, 349.
(7) Zaikin, A. N.; Zhabotinsky, A. M. *Nature* **1970**, *225*, 535.
(8) Winfree, A. T. *Science* **1972**, *175*, 634.
(9) Plesser, Th.; Müller, S. C.; Hess, B. *J. Phys. Chem.* **1990**, *94*, 7501.
(10) Kuhnert, L. *Naturwissenschaften* **1986**, *73*, 96.
(11) Agladze, K. I.; Davydov, V. A.; Mikhailov, A. S. *JETP Lett.* **1987**, *45*, 767.
(12) Steinbock, O.; Zykov, V. S.; Müller, S. C. *Nature* **1993**, *366*, 322.
(13) Braune, M.; Engel, H. *Chem. Phys. Lett.* **1993**, *211*, 534.
(14) Zykov, V. S.; Steinbock, O.; Müller, S. C. *Chaos* **1994**, *4*, 509.
(15) Braune, M.; Schrader, A.; Engel, H. *Chem. Phys. Lett.* **1994**, *222*, 358.
(16) Grill, S.; Zykov, V. S.; Müller, S. C. *Phys. Rev. Lett.* **1995**, *75*, 3369.
(17) Yamaguchi, T.; Kuhnert, L.; Nagy-Ungvarai, Zs.; Müller, S. C.; Hess, B. *J. Phys. Chem.* **1991**, *95*, 5831.
(18) Jahnke, W.; Winfree, A. T. *Int. J. Bifurcation and Chaos* **1991**, *1*, 445.
(19) Müller, S. C.; Plesser, Th.; Hess, B. *Physica D* **1987**, *24*, 71.
(20) Steinbock, O.; Müller, S. C. *Physica A* **1992**, *188*, 61.
(21) Zykov, V. S. *Simulation of Wave Processes in Excitable Media*; Manchester University Press: Manchester, 1987.
(22) Jahnke, W.; Skaggs, W. E.; Winfree, A. T. *J. Phys. Chem.* **1989**, *93*, 740.
(23) Skinner, G. S.; Swinney, H. L. *Physica D* **1990**, *48*, 1.
(24) Field, R. J.; Körös, E.; Noyes, R. M. J. *J. Am. Chem. Soc.* **1972**, *94*, 8649.
(25) Tyson, J. J. In *Oscillations and Travelling Waves in Chemical Systems*; Field, R., Burger, M., Eds.; Wiley: New York, 1985; p 93.
(26) Davydov, V. A.; Zykov, V. S.; Mikhailov, A. S. *Sov. Phys. Usp.* **1991**, *34*, 665.
(27) Guevara, M. R.; Glass, L.; Shrier, A. *Science* **1981**, *214*, 1350.
(28) Ross, J.; Pugh, S.; Schell, M. In *From Chemical to Biological Organization*; Markus, M., Müller, S. C., Nicolis, G., Eds.; Springer: Berlin, 1988; p 34.
(29) DeYoung, G.; Othmer, H. G. *Ann. N.Y. Acad. Sci.* **1990**, *591*, 128.

JP9616674